Influence of molecular conformations on the electronic structure of organic charge transfer salts

Daniel Guterding,* Roser Valentí, and Harald O. Jeschke
Institut für Theoretische Physik, Goethe-Universität Frankfurt, Max-von-Laue-Straße 1, 60438 Frankfurt am Main, Germany

We report *ab-initio* calculations for the electronic structure of organic charge transfer salts κ-$(ET)_2Cu[N(CN)_2]Br$, κ-$(ET)_2Cu[N(CN)_2]I$, κ''-$(ET)_2Cu[N(CN)_2]Cl$ and κ-$(ET)_2Cu_2(CN)_3$. These materials show an ordering of the relative orientation of terminal ethylene groups in the BEDT-TTF molecules at finite temperature and our calculations correctly predict the experimentally observed ground state molecular conformations (eclipsed or staggered). Further, it was recently demonstrated that the ethylene endgroup relative orientations can be used to reversibly tune κ-$(ET)_2Cu[N(CN)_2]Br$ through a metal-insulator transition. Using a tight-binding analysis, we show that the molecular conformations of ethylene endgroups are intimately connected to the electronic structure and significantly influence hopping and Hubbard repulsion parameters. Our results place κ-$(ET)_2Cu[N(CN)_2]Br$ in eclipsed and staggered configurations on opposite sides of the metal-insulator transition.

PACS numbers: 71.10.Fd, 71.15.Mb, 71.20.Rv, 74.70.Kn

Quasi-two dimensional charge transfer salts κ-$(BEDT\text{-}TTF)_2X$, where BEDT-TTF stands for bis-ethylenedithio-tetrathiafulvalene, often abbreviated as ET, constitute a fascinating family of materials due to their rich phase diagrams comprising metallic, superconducting, Mott insulating and spin-liquid phases [1–4].

These electronic properties of ET-based materials are very sensitive to disorder. Irradiation experiments have shown that lattice disorder lowers the T_c of κ-$(ET)_2Cu(SCN)_2$ [5] and causes electron localization in κ-$(ET)_2Cu[N(CN)_2]Br$ [6]. Early on it was also realized that ET molecules have intramolecular degrees of freedom, namely the configurations of their two ethylene endgroups (see Fig. 3), which can either be aligned parallel (eclipsed, E) or canted (staggered, S) [7–17]. The energetically favorable configuration is not universal for different anions X and packing motifs. For some materials a glass-like freezing of the ethylene endgroups upon cooling has been observed [7, 8, 15–19].

Especially the first ambient pressure ET-based superconductor β-$(ET)_2I_3$ attracted a lot of interest, because its T_c can be enhanced from 1.5 K to 8 K by forcing the ET molecules, which are endgroup disordered at ambient pressure, to assume staggered configuration through application of shear and pressure [7–11, 20, 21]. Recently, it was shown that ethylene endgroup disorder can be used to reversibly tune κ-$(ET)_2Cu[N(CN)_2]Br$ through a metal to insulator transition [17, 22, 23].

It is believed that materials κ-$(ET)_2X$ have a common phase diagram, which is mainly controlled by the value of the on-site Coulomb repulsion U over the electronic bandwidth [24]. Changes in physical properties in the presence of ethylene endgroup disorder have so far been interpreted as a consequence of lattice disorder, with the exception of recent scanning tunneling spectroscopy experiments [25]. Surprisingly, the effect of different ethylene endgroup configurations on the electronic structure, and especially the electronic bandwidth, of κ-$(ET)_2X$ has only been investigated in a single material using the extended Hückel method [13], while calculations for ET molecules and dimers in vacuum are available [17, 26, 27]. A preceding study for κ-$(ET)_2Cu[N(CN)_2]Br$ focused on energetics rather than bandstructure effects [16].

Here we examine the electronic structure of endgroup *ordered* crystals in both possible configurations for various members of the κ-$(ET)_2X$ family of materials using *ab-initio* density functional theory (DFT) calculations. We construct a 3/4-filled low-energy effective Hamiltonian using a Wannier downfolding scheme and relate the resulting model parameters to the relative orientation of terminal ethylene groups. Our results show that ethylene endgroup configurations of ET molecules influence the electronic bandwidth of all resulting crystalline materials investigated here. Finally, we offer a simplified interpretation of our results in terms of the Hubbard model on the anisotropic triangular lattice and relate our findings to recent experiments, especially pointing out the possibility that changes in the electronic structure through ethylene endgroup disorder and strongly enhanced electron correlation are relevant in addition to commonly considered lattice disorder.

We used *ab-initio* density functional theory (DFT) calculations within an all-electron full-potential local orbital (FPLO) [28] basis to calculate the electronic bandstructure. For the exchange-correlation functional we employed the generalized gradient approximation (GGA) [29]. All calculations were converged on $6 \times 6 \times 6$ k-point grids.

Tight-binding models were obtained from projective molecular orbital Wannier functions as implemented in FPLO [30]. We have shown previously that, for the materials of interest here, this method yields near per-

fect representations of the low-energy DFT bandstructure and avoids ambiguities from band fitting procedures [31]. The resulting tight-binding Hamiltonian $H = \sum_{ij\sigma} t_{ij}(c^\dagger_{i\sigma}c_{j\sigma} + h.c.)$ is 3/4-filled and consists of four bands corresponding to the four ET sites indexed by i, j. Each site is located at the center of the inner C-C bond of an ET molecule. Subsequently, we relate those *ab-initio* calculated parameters with an effective two-band half-filled Hubbard model on the anisotropic triangular lattice.

Experimental crystal structures including both possible ethylene endgroup configurations are available [12, 32, 33] for κ-$(ET)_2Cu[N(CN)_2]I$, κ''-$(ET)_2Cu[N(CN)_2]Cl$ and κ-$(ET)_2Cu_2(CN)_3$ ($T = 200$ K), while for κ-$(ET)_2Cu[N(CN)_2]Br$ only one endgroup configuration has been reported in the literature [12]. For the latter case, we set up the missing ethylene endgroup orientation by hand. For κ-$(ET)_2Cu[N(CN)_2]I$ we used the crystal structure determined at $T = 127$ K if not denoted otherwise. The structure at $T = 295$ K is used as a consistency check.

In Figure 1 we show as an example the displacement ellipsoids resulting from the structure determination of κ''-$(ET)_2Cu[N(CN)_2]Cl$. These represent the uncertainty of the experimentally determined structure with respect to the position of every individual atom. Displacements on the endgroup carbon atoms are largest, but the uncertainty of the sulphur atom positions next to the ethylene endgroups is also significant. Therefore, we chose to relax the entire ethylene endgroups together with the two neighboring sulphur atoms in both staggered and eclipsed endgroup configurations for all materials investigated here. For comparison of the relaxed crystal structures with eclipsed and staggered endgroups see Fig. 3. Other atomic positions and the unit cell parameters were left untouched. Note that hydrogen positions belonging to the ethylene groups were not measured in experiment and had to be inserted manually.

For the structural relaxation we used the projector augmented wave (PAW) method [34] as implemented in GPAW [35]. We optimized the terminal ethylene endgroups using $2 \times 2 \times 2$ k-point grids and GGA exchange-correlation functional until forces were below 10 meV/Å.

It turns out that both endgroup configurations locally minimize the total DFT energy, so that stable crystal structures can be obtained for both staggered and eclipsed orientations from a DFT relaxation.

It is experimentally known that different charge transfer salts can either have staggered or eclipsed endgroups as their lowest energy configuration. To confirm the validity of our relaxed structures, we first calculate the energy difference ΔE between staggered and eclipsed using FPLO. The results are displayed in Table I. Values for the energy differences calculated with GPAW are in good agreement. The energy ordering of staggered and eclipsed configurations comes out correctly

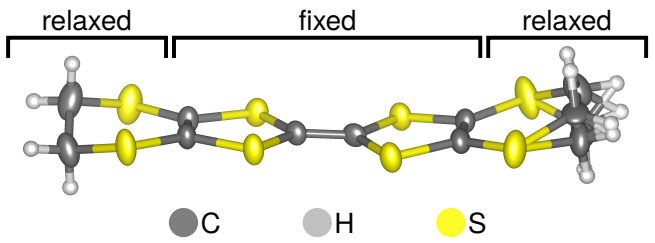

FIG. 1. (Color online) ET molecule with displacement ellipsoids from the experimental structure determination of κ''-$(ET)_2Cu[N(CN)_2]Cl$. The size of the ellipsoids scales with the amount of uncertainty regarding the respective atomic position. Ethylene endgroup disorder is included on the right end of the molecule and given by fractionally occupied positions. The bars above the molecule indicate which parts of the ET molecules are relaxed in our DFT calculations and which atomic positions remain at their experimental values.

TABLE I. Lowest energy configurations of the ethylene endgroups determined from our DFT relaxed structures. The energy difference ΔE to the high energy configuration is calculated per ET molecule from the FPLO total energies.

	configuration	ΔE in meV
κ-$(ET)_2Cu_2(CN)_3$	staggered	130
κ''-$(ET)_2Cu[N(CN)_2]Cl$	eclipsed	72
κ-$(ET)_2Cu[N(CN)_2]Br$	eclipsed	110
κ-$(ET)_2Cu[N(CN)_2]I$	staggered	38

for all investigated materials with the exception of κ-$(ET)_2Cu[N(CN)_2]I$ at 295K, where the energy difference is the smallest and the distribution of endgroup configurations measured experimentally was found to be 51:49 [12, 32, 33]. The value for ΔE we determined is the energy difference between the two local minima of the energy corresponding to staggered and eclipsed configurations, which is not to be confused with the activation energy. The latter denotes the height of the potential barrier between those minima, which can be significantly larger than ΔE [14, 22]. Instead, our DFT calculated values constitute a lower bound for the activation energy: κ-$(ET)_2Cu[N(CN)_2]I$ with the smallest energy difference is known to be completely endgroup disordered at room temperature [12] and κ''-$(ET)_2Cu[N(CN)_2]Cl$ contains about 20% disorder at room temperature [32], while in the other two materials the amount of endgroup disorder is in a range of few percent.

The electronic bandstructures obtained from the molecular Wannier function analysis of the DFT results are shown in Fig. 2 for both eclipsed and staggered ethylene endgroup configurations. In all bandstructures shown, the difference between staggered and eclipsed configurations lies in the electronic bandwidth. Going from eclipsed to staggered, the overall bandwidth increases, while the width of the two bands closest to the Fermi level decreases.

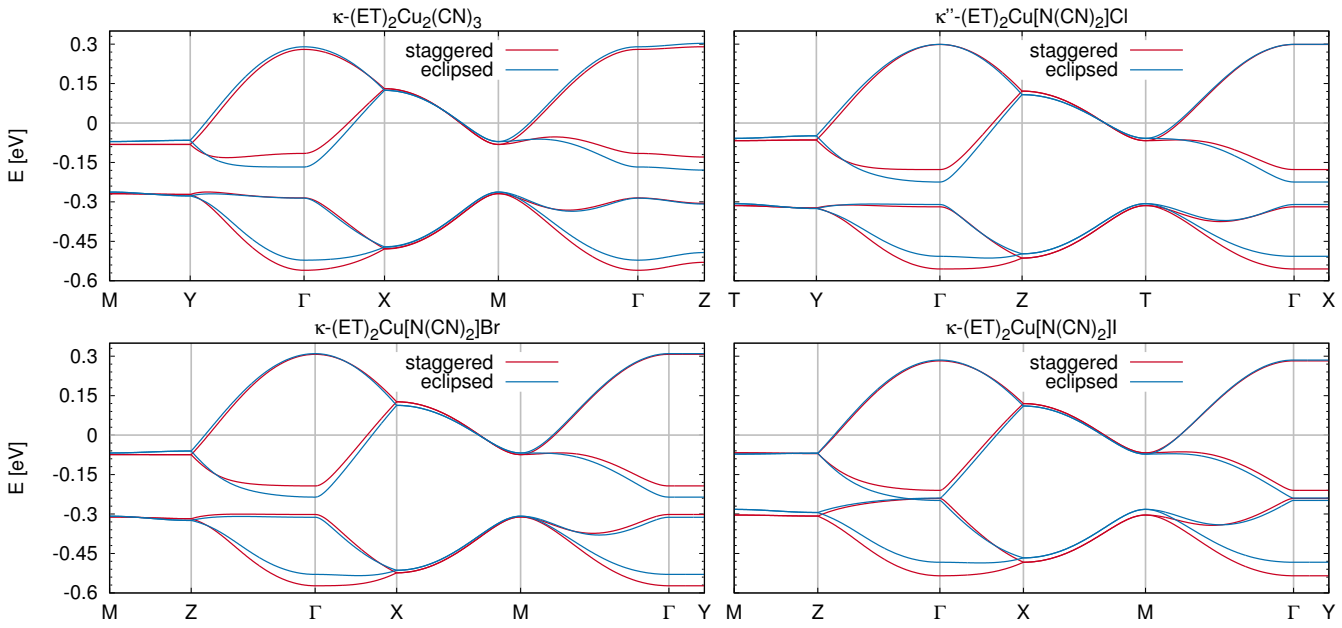

FIG. 2. (Color online) Electronic bandstructure of all investigated materials for staggered and eclipsed ethylene endgroup configurations. Staggered ethylene endgroups produce a larger overall bandwidth than eclipsed ones, but reduce the width of the two bands closest to the Fermi level.

We analyse these bandstructures using a minimal model [36] for a κ-packed layer of individual ET molecules (Fig. 3) using the four largest parameters (t_1,t_2,t_3,t_4) also commonly denoted as (b_1,p,b_2,q). Note that our tight binding Hamiltonians also include small longer range hoppings. The four largest hopping parameters are given in Tab. II. Parameters t_1 (b_1) and t_3 (b_2) decrease from staggered to eclipsed configurations, while t_4 (q) increases and t_2 (p) remains about constant.

The molecular Wannier functions for an ET molecule in eclipsed and staggered configuration are shown in Fig. 3. Although the molecular Wannier function hardly resides on the terminal ethylene groups, overlaps with neighboring ET molecules are influenced by the configuration of the endgroups through the direction of their bonds with the neighboring sulphur atoms.

Especially the hopping t_3 is strongly enhanced, because the tails of the Wannier function on the neighboring ET molecule are enlarged. The Wannier functions remain largely unaltered in the direction that corresponds to t_2. Therefore, this parameter largely remains constant. In the direction of t_4 the tail on the neighboring ET molecule is enhanced in the staggered configuration, but the Wannier function on the central molecule turns away from this tail because of the altered suplhur-ethylene bond direction. Consequently, t_4 is reduced. The relative changes in t_1 are rather small, which is consistent with our analysis of the Wannier functions.

The effect of the altered hopping integrals and its connection to the metal-insulator transition in κ-(ET)$_2$Cu[N(CN)$_2$]Br can also be understood in terms of

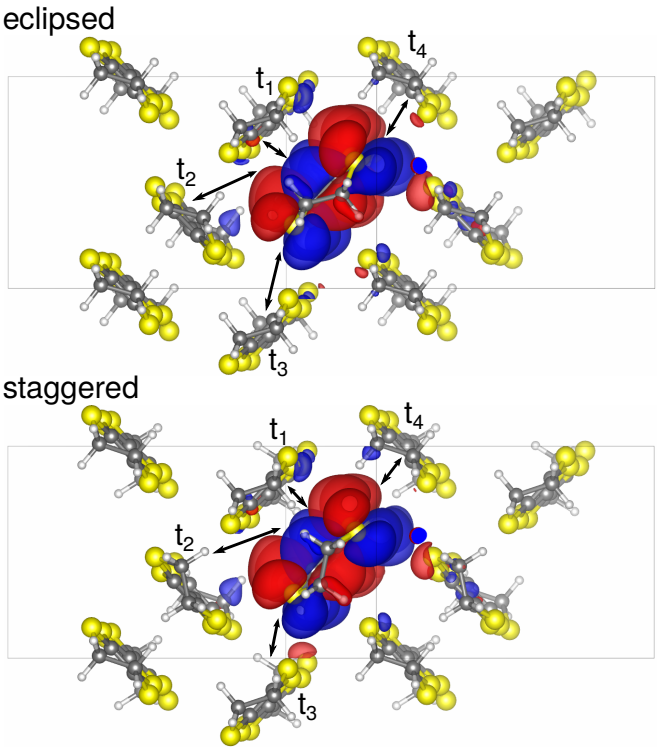

FIG. 3. (Color online) Molecular Wannier function of an ET molecule in staggered and eclipsed configuration for κ-(ET)$_2$Cu[N(CN)$_2$]Br. The arrows denote the directions of dominant hopping processes in the individual molecule model with (t_1,t_2,t_3,t_4).

TABLE II. Values of the molecule model parameters (t_1,t_2,t_3,t_4) in meV, also commonly denoted as (b_1,p,b_2,q). Dimer model parameters are given as ratios t'/t and U/t calculated from (t_1,t_2,t_3,t_4) using formulas described in the text. The second column states the experimental ground state of the respective material (I=insulator, M=metal, SC=superconductor). The x in the fourth column marks the low energy configuration of the ethylene endgroups.

				t_1	t_2	t_3	t_4	t'/t	U/t
κ-(ET)$_2$Cu$_2$(CN)$_3$	I	eclipsed		167	84.9	70.4	30.3	0.61	5.8
		staggered	x	176	78.0	81.4	18.7	0.84	7.3
κ''-(ET)$_2$Cu[N(CN)$_2$]Cl	M	eclipsed	x	174	97.3	50.5	35.9	0.38	5.2
		staggered		188	93.4	64.0	26.6	0.53	6.3
κ-(ET)$_2$Cu[N(CN)$_2$]Br	SC	eclipsed	x	178	99.0	59.5	35.8	0.44	5.3
		staggered		187	97.1	70.2	24.9	0.58	6.1
κ-(ET)$_2$Cu[N(CN)$_2$]I, 127 K	M	eclipsed		152	101	47.2	29.2	0.36	4.7
		staggered	x	170	99.0	52.4	18.9	0.44	5.8
κ-(ET)$_2$Cu[N(CN)$_2$]I, 295 K	M	eclipsed		153	92.0	49.9	31.5	0.40	4.9
		staggered		164	92.0	54.8	22.2	0.48	5.8

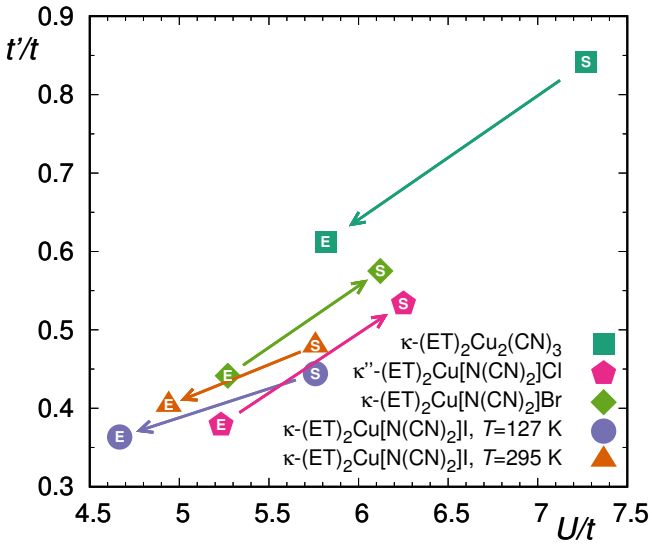

FIG. 4. (Color online) Parameter ratios t'/t and U/t in the effective dimer model. The direction of the arrows indicates the direction of change in the model parameters going from the low to the high energy configuration of the ethylene endgroups. Eclipsed (E) endgroup configurations are located on the left side (small U/t) of the plot, while staggered (S) endgroup configurations are located on the right side (large U/t).

the simplified two-band dimer model. We calculate the parameters t, t' and U of the corresponding anisotropic triangular lattice Hubbard from the usual geometric formulas $t = (|t_2| + |t_4|)/2$, $t' = |t_3|/2$ and use the rough estimate $U \approx 2|t_1|$ for the intradimer Hubbard repulsion [36, 37].

Recently, there has been some criticism of this method of obtaining a t, t' and U dimer model, because the estimate for U relies on the fact that the unscreened intermolecular Coulomb repulsion V_1 within an (ET)$_2$ dimer vanishes. In DFT parametrizations of this model V_1 was however found to be non-negligible [26, 27, 38].

Calculations based on the constrained random phase approximation additionally showed sizeable screening effects [39] in the dimer approximated model not accounted for in our method. In iron-based materials it is however a well-known problem that different, even very sophisticated, approximations made in the determination process can lead to wildly different parameter sets [40–42].

Recent Wannier function analysis anyway points to the fact that a 3/4-filled Hubbard model of individual ET-molecules is more appropriate to understand fine details of κ-ET materials [31, 43]. Unfortunately, there are only few examples of many-body calculations based on such multi-band Hamiltonias [44, 45]. Alternatively, a half-filled extended Hubbard model including non-local Coulomb repulsion and exchange interactions has been proposed [46].

We however emphasize that so far dimer approximated Hamiltonians and subsequent many-body calculations showed remarkable success in explaining some of the qualitative properties of ET based materials [47, 48] and should be sufficient for the case we investigate here. Note that our estimates agree especially well with more elaborate calculations including screening effects [39, 49]. Newly discovered effects like multiferroic behavior [50] or the still unsettled nature of superconductivity [45, 51] however certainly call for more realistic approaches.

Fig. 4 shows the result of our dimer model estimate. The change from eclipsed to staggered ethylene group configuration universally increases both the frustration t'/t and the relative strength of the Hubbard repulsion U/t, i.e. U over the bandwidth.

Comparison of our findings with cellular dynamical mean-field theory [47] and exact diagonalization results for the anisotropic triangular lattice Hubbard model [48] explains why κ-(ET)$_2$Cu[N(CN)$_2$]Br can be tuned into a Mott insulating state by activating [22, 23] the energetically less favorable endgroup configuration: First, the material in its lowest energy configuration is already close to a Mott insulating phase. Second, the lowest energy configuration is the eclipsed one, so U/t can be

strongly increased by activating the staggered configuration. Therefore, the system crosses the phase transition line and a Mott insulator is realized.

Note that the phase diagram of the anisotropic triangular lattice Hubbard model is not entirely settled and slightly different results have been obtained using other numerical methods [52, 53].

In conclusion, we demonstrated that DFT reliably reproduces the ground state ethylene endgroup configuration for various κ-phase materials. While previous discussion of endgroup conformations in the literature considered only lattice disorder a relevant issue, we have shown that the relative orientation of ethylene endgroups within ET molecules crucially influences the electronic bandwidth of κ-type organic charge transfer salts. Switching an ET molecule from eclipsed to staggered configuration decreases the electronic bandwidth and in turn enhances the relative strength of the Hubbard repulsion, bringing the material closer to a Mott insulating state. Recent experiments where κ-$(ET)_2Cu[N(CN)_2]Br$ was reversibly switched from a metallic to an insulating state by tuning the endgroup configurations are easily understood in our picture. In κ-type materials that are not close to any phase transition, the effects of ethylene endgroup disorder might not manifest as dramatically as in κ-$(ET)_2Cu[N(CN)_2]Br$. Based on our estimates of model parameters, κ''-$(ET)_2Cu[N(CN)_2]Cl$ might exhibit similar behavior.

The authors would like to thank Benedikt Hartmann and Jens Müller for pointing this interesting problem out to us and acknowledge support by the Deutsche Forschungsgemeinschaft through grant SFB/TR 49. Calculations were performed on the LOEWE-CSC and FUCHS supercomputers of the Center for Scientific Computing (CSC) in Frankfurt am Main, Germany.

* guterding@itp.uni-frankfurt.de

[1] H. Elsinger, J. Wosnitza, S. Wanka, J. Hagel, D. Schweitzer, and W. Strunz, *κ-(BEDT-TTF)$_2$Cu[N(CN)$_2$]Br: A Fully Gapped Strong-Coupling Superconductor*, Phys. Rev. Lett. **84**, 6098 (2000).

[2] Y. Shimizu, K. Miyagawa, K. Kanoda, M. Maesato, and G. Saito, *Spin Liquid State in an Organic Mott Insulator with a Triangular Lattice*, Phys. Rev. Lett. **91**, 107001 (2003).

[3] Y. Kurosaki, Y. Shimizu, K. Miyagawa, K. Kanoda, and G. Saito, *Mott Transition from a Spin Liquid to a Fermi Liquid in the Spin-Frustrated Organic Conductor κ-(ET)$_2$Cu$_2$(CN)$_3$*, Phys. Rev. Lett. **95**, 177001 (2005).

[4] F. Kagawa, K. Miyagawa, and K. Kanoda, *Unconventional critical behaviour in a quasi-two-dimensional organic conductor*, Nature (London) **436**, 534 (2005).

[5] J. G. Analytis, A. Ardavan, S. J. Blundell, R. L. Owen, E. F. Garman, C. Jeynes, and B. J. Powell, *Effect of Irradiation-Induced Disorder on the Conductivity and Critical Temperature of the Organic Superconductor κ-(BEDT-TTF)$_2$Cu(SCN)$_2$*, Phys. Rev. Lett. **96**, 177002 (2006).

[6] K. Sano, T. Sasaki, N. Yoneyama, and N. Kobayashi, *Electron Localization near the Mott transition in the Organic Superconductor κ-(BEDT-TTF)$_2$Cu[N(CN)$_2$]Br*, Phys. Rev. Lett. **104**, 217003 (2010).

[7] P. W. C. Leung, T. J. Emge, M. A. Beno, H. H. Wang, and J. M. Williams, *Novel Structural Modulation in the First Ambient-Pressure Sulfur-Based Organic Superconductor (BEDT-TTF)$_2$I$_3$*, J. Am. Chem. Soc. **106**, 7644 (1984).

[8] P. W. Leung, T. J. Emge, M. A. Beno, H. H. Wang, J. M. Williams, V. Petricek, and P. Coppens, *Novel Structural Modulation in the Ambient-Pressure Sulfur-Based Organic Superconductor β-(BEDT-TTF)$_2$I$_3$: Origin and Effects on Its Electrical Conductivity*, J. Am. Chem. Soc. **107**, 6184 (1985).

[9] A. J. Schultz, H. H. Wang, and J. M. Williams, *Effect of Structural Disorder on Organic Superconductors: A Neutron Diffraction Study of "High-T_c" β^*-(BEDT-TTF)$_2$I$_3$ at* 4.5 K *and* 1.5 kbar, J. Am. Chem. Soc. **108**, 7853 (1986).

[10] A. J. Schultz, M. A. Beno, H. H. Wang, and J. M. Williams, *Neutron-diffraction evidence for ordering in the high-T_c phase of β-di[bis(ethylenedithio)tetrathiafulvalene]triiodide [β^*-(ET)$_2$I$_3$]*, Phys. Rev. B **33**, 7823 (1986).

[11] J. E. Schirber, L. J. Azevedo, J. F. Kwak, E. L. Venturini, P. C. W. Leung, M. A. Beno, H. H. Wang, and J. M. Williams, *Shear-induced superconductivity in β-di[-Bis(ethylene- dithio)tetrathiafulvalene]triiodide [β-(BEDT-TTF)$_2$I$_3$]*, Phys. Rev. B **33**, 1987 (1986).

[12] U. Geiser, A. J. Schultz, H. W. Wang, D. M. Watkins, D. L. Stupka, J. M. Williams, J. E. Schirber, D. L. Overmeyer, D. Jung, J. J. Novoa, and M.-H. Whangbo, *Strain index, lattice softness and superconductivity of organic donor-molecule salts, Crystal and electronic structures of three isostructural salts κ-(BEDT-TTF)$_2$Cu[N(CN)$_2$]X (X = Cl, Br, I)*, Physica C **174**, 475 (1990).

[13] Masashi Watanabe, *Low temperature structures and insulating phases in quasi two-dimensional charge transfer salts at 3/4 filling*, Ph.D. Thesis (in Japanese), Graduate School of Natural Science and Technology, Okayama University, Japan (1999).

[14] J. Müller, M. Lang, F. Steglich, J. A. Schlueter, A. M. Kini, and T. Sasaki, *Evidence for structural and electronic instabilities at intermediate temperatures in κ-(BEDT-TTF)$_2$X for X=Cu[N(CN)$_2$]Cl, Cu[N(CN)$_2$]Br and Cu(NCS)$_2$: Implications for the phase diagram of these quasi-two-dimensional organic superconductors*, Phys. Rev. B **65**, 144521 (2002).

[15] N. Toyota, M. Lang, J. Müller *Low-Dimensional Molecular Metals*, Springer-Verlag Berlin Heidelberg 2007.

[16] A. Aburto and E. Orgaz, *Ab initio electronic structure of the eclipsed and staggered conformations of the κ-(BEDT-TTF)$_2$Cu[N(CN)$_2$]Br organic superconductor*, Phys. Rev. B **78**, 113104 (2008).

[17] J. Müller, B. Hartmann, R. Rommel, J. Brandenburg, S. M. Winter, and J. A. Schlueter, *Origin of the glass-like dynamics in molecular metals κ-(BEDT-TTF)$_2$X: implications from fluctuation spectroscopy and ab-initio calculations*, arXiv:1506.05191 (unpublished).

[18] K. Saito, H. Akutsu, M. Sorai, *Glass transition in the or-*

ganic superconductor with the highest T_c under ambient pressure, κ-(BEDT-TTF)$_2$Cu[N(CN)$_2$]Br, Solid State Commun. **111**, 471 (1999).

[19] H. Akutsu, K. Saito, M. Sorai, *Phase behavior of the organic superconductors κ-(BEDT-TTF)$_2$Cu[N(CN)$_2$]Br and Cl studied by ac calorimetry*, Phys. Rev. B **61**, 4346 (2000).

[20] V. N. Tauklin, E. E. Kostyuchenko, Yu. V. Sushko, I. F. Shchegolev, and E. B. Yagubskii, *Effect of pressure on the superconductivity of β-(BEDT-TTF)$_2$I$_3$*, Pis'ma Zh. Eksp. Theor. Fiz. **41**, 68 (1984) [JETP Lett. **41**, 81 (1985)].

[21] K. Murata, M. Tokumoto, H. Anzai, H. Bando, G. Saito, K. Kajimura, and T. Ishiguro, *Superconductivity with the Onset at* 8 K *in the Organic Conductor β-(BEDT-TTF)$_2$I$_3$ under Pressure*, J. Phys. Soc. Jpn. **54**, 1236 (1985).

[22] B. Hartmann, J. Müller, and T. Sasaki, *Mott metal-insulator transition induced by utilizing a glasslike structural ordering in low-dimensional molecular conductors*, Phys. Rev. B **90**, 195150 (2014).

[23] B. Hartmann, D. Zielke, J. Polzin, T. Sasaki, and J. Müller, *Critical Slowing Down of the Charge Carrier Dynamics at the Mott Metal-Insulator Transition*, Phys. Rev. Lett. **114**, 216403 (2015).

[24] K. Kanoda, *Electron Correlation, Metal-Insulator Transition and Superconductivity in Quasi-2D Organic Systems, (ET)$_2$X*, Physica C **282-287**, 299 (1997).

[25] S. Diehl, T. Methfessel, U. Tutsch, J. Müller, M. Lang, M. Huth, M. Jourdan, and H.-J. Elmers, *Disorder-induced gap in the normal density of states of the organic superconductor κ-(BEDT-TTF)$_2$Cu[N(CN)$_2$]Br*, J. Phys.: Condens. Matter **27**, 265601 (2015).

[26] E. Scriven and B. J. Powell, *Toward parametrization of the Hubbard model for salts of bis(ethylenedithio)tetrathiafulvalene: A density functional study of isolated molecules*, Journal of Chemical Physics **130**, 104508 (2009).

[27] E. Scriven and B. J. Powell, *Effective Coulomb interactions within BEDT-TTF dimers*, Phys. Rev. B **80**, 205107 (2009).

[28] K. Koepernik and H. Eschrig, *Full-potential nonorthogonal local-orbital minimum-basis band-structure scheme*, Phys. Rev. B **59**, 1743 (1999); http://www.FPLO.de

[29] J. P. Perdew, K. Burke, and M. Ernzerhof, *Generalized Gradient Approximation Made Simple*, Phys. Rev. Lett. **77**, 3865 (1996).

[30] H. Eschrig and K. Koepernik, *Tight-binding models for the iron-based superconductors*, Phys. Rev. B **80**, 104503 (2009).

[31] M. Altmeyer, R. Valentí, and H. O. Jeschke, *Role of layer packing for the electronic properties of the organic superconductor (BEDT-TTF)$_2$Ag(CF$_3$)$_4$(TCE)*, Phys. Rev. B **91**, 245137 (2015).

[32] N. D. Kushch, A. V. Kazakova, L. I. Buravov, A. N. Chekhlov, A. D. Dubrovskii, E. B. Yagubskii, and E. Canadell, *The first polymorph, κ''-(ET)$_2$Cu[N(CN)$_2$]Cl, in the family of κ-(ET)$_2$Cu[N(CN)$_2$]X (X = Cl, Br, I) radical cation salts*, Journal of Solid State Chemistry **182**, 617 (2009).

[33] H. O. Jeschke, M. de Souza, R. Valentí, R. S. Manna, M. Lang, and J. A. Schlueter, *Temperature dependence of structural and electronic properties of the spin-liquid candidate κ-(BEDT-TTF)$_2$Cu$_2$(CN)$_3$*, Phys. Rev. B **85**, 035125 (2012).

[34] P. E. Blöchl, *Projector augmented-wave method*, Phys. Rev. B **50**, 17953 (1994).

[35] J. Enkovaara, C. Rostgaard, J. J. Mortensen *et al.*, *Electronic structure calculations with GPAW: a real-space implementation of the projector augmented-wave method*, J. Phys.: Condens. Matter **22**, 253202 (2010); https://wiki.fysik.dtu.dk/gpaw

[36] T. Komatsu, N. Matsukawa, T. Inoue, and G. Saito, *Realization of Superconductivity at Ambient Pressure by Band-Filling Control in κ-(BEDT-TTF)$_2$Cu$_2$(CN)$_3$*, J. Phys. Soc. Jpn. **65**, 1340 (1996).

[37] M. Tamura, H. Tajima, K. Yakushi, H. Kuroda, A. Kobayashi, R. Kato, and H. Kobayashi, *Reflectance Spectra of κ-(BEDT-TTF)$_2$I$_3$: Electronic Structure of Dimeric BEDT-TTF Salts*, J. Phys. Soc. Jpn. **60**, 3861 (1991).

[38] Y. Imamura, S. Ten-no, K. Yonemitsu, and Y. Tanimura, *Structures and electronic phases of the bis(ethylenedithio)tetrathiafulvalene (BEDT-TTF) clusters and κ-(BEDT-TTF) salts: A theoretical study based on ab initio molecular orbital methods*, J. Chem. Phys. **111**, 5986 (1999).

[39] K. Nakamura, Y. Yoshimoto, T. Kosugi, R. Arita, and M. Imada, *Ab initio Derivation of Low-Energy Model for κ-ET Type Organic Conductors*, J. Phys. Soc. Jpn. **78**, 083710 (2009).

[40] V. I. Ansimov, D. M. Korotin, A. V. Kozhevnikov, J. Kuneš, A. O. Shorikov, S. L. Skornyakov, and S. V. Streltsov, *Coulomb repulsion and correlation strength in LaFeAsO from density functional and dynamical mean-field theories*, J. Phys.: Condens. Matter **21**, 075602 (2009).

[41] M. Aichhorn, L. Pourovskii, V. Vildosola, M. Ferrero, O. Parcollet, T. Miyake, A. Georges, and S. Biermann, *Dynamical mean-field theory within an augmented plane-wave framework: Assessing electronic correlations in the iron pnictide LaFeAsO*, Phys. Rev. B **80**, 085101 (2009).

[42] A. Kutepov, K. Haule, S. Y. Savrasov, and G. Kotliar, *Self-consistent GW determination of interaction strength: Application to the iron arsenide superconductors*, Phys. Rev. B **82**, 045105 (2010).

[43] T. Koretsune and C. Hotta, *Evaluating model parameters of the κ- and β′-type Mott insulating organic solids*, Phys. Rev. B **89**, 045102 (2014).

[44] J. Ferber, K. Foyevtsova, H. O. Jeschke, and R. Valentí, *Unveiling the microscopic nature of correlated organic conductors: The case of κ-(ET)$_2$Cu[N(CN)$_2$]Br$_x$Cl$_{1-x}$*, Phys. Rev. B **89**, 205106 (2014).

[45] K. Kuroki, T. Kimura, R. Arita, Y. Tanaka, and Y. Matsuda, *$d_{x^2-y^2}$- versus d_{xy}-like pairings in organic superconductors κ-(BEDT-TTF)$_2$X*, Phys. Rev. B **65**, 100516(R) (2002).

[46] H. Shinaoka, T. Misawa, K. Nakamura, and M. Imada, *Mott Transition and Phase Diagram of κ-(BEDT-TTF)$_2$Cu(NCS)$_2$ Studied by Two-Dimensional Model Derived from Ab initio Method*, J. Phys. Soc. Jpn. **81**, 034701 (2012).

[47] B. Kyung and A.-M. S. Tremblay, *Mott Transition, Antiferromagnetism, and d-Wave Superconductivity in Two-Dimensional Organic Conductors*, Phys. Rev. Lett. **97**, 046402 (2006).

[48] R. T. Clay, H. Li, and S. Mazumdar, *Absence of Superconductivity in the Half-Filled Band Hubbard Model on*

the Anisotropic Triangular Lattice, Phys. Rev. Lett. **101**, 166403 (2008).

[49] H. C. Kandpal, I. Opahle. Y.-Z. Zhang, H. O. Jeschke, R. Valentí, *Revision of Model Parameters for κ-Type Charge Transfer Salts: An Ab Initio Study*, Phys. Rev. Lett. **103**, 067004 (2009).

[50] P. Lunkenheimer, J. Müller, S. Krohns, F. Schrettle, A. Loidl, B. Hartmann, R. Rommel, M. de Souza, C. Hotta, J. A. Schlueter, and M. Lang, *Multiferroicity in an organic charge-transfer salt that is suggestive of electric-dipole-driven magnetism*, Nat. Mater. **11**, 755 (2012).

[51] A. Ardavan, S. Brown, S. Kagoshima, K. Kanoda, K. Kuroki, H. Mori, M. Ogata, S. Uji, and J. Wosnitza, *Recent Topics of Organic Superconductors*, J. Phys. Soc. Jpn. **81**, 011004 (2012).

[52] H. Morita, S. Watanabe, and M. Imada, *Nomagnetic Insulating States near the Mott Transitions on Lattices with Geometrical Frustration and Implications for κ-(ET)$_2$Cu$_2$(CN)$_3$*, J. Phys. Soc. Jpn. **71**, 2109 (2002).

[53] T. Koretsune, Y. Motome, and A. Furusaki, *Exact Diagonalization Study of Mott Transition in the Hubbard Model on an Anisotropic Triangular Lattice*, J. Phys. Soc. Jpn. **76**, 074719 (2007).